*Friction* https://mc03.manuscriptcentral.com/friction
https://doi.org/10.26599/FRICT.2026.9441232

Research Article

# A novel rolling contact fatigue testing method based on dry-wet alternation and damage mechanism of rails

Honghao Wang[1], Haohao Ding[1], Qunli Zhang[2], Qian Xiao[3], Wenjian Wang[1], Shuyue Zhang[1], Qiyue Liu[1], Zhongrong Zhou[1]

[1] *Tribology Research Institute, State Key Laboratory of Traction Power, Southwest Jiaotong University, Chengdu 610031, China*

[2] *Institute of Laser Advanced Manufacturing, Zhejiang University of Technology, Hangzhou 310023, China*

[3] *State Key Laboratory of Performance Monitoring Protecting of Rail Transit Infrastucture, East China Jiaotong University, Nanchang 330013, China*

[*] Corresponding author: Shuyue Zhang, E-mail: zhangsy@swjtu.edu.cn



Received: July 4, 2024; Revised: January 4, 2026; Accepted: February 7, 2026



**Abstract:** Rolling contact fatigue (RCF) damage is the critical damage form faced by rails, especially under rainy and humidity conditions. In order to deeply explore the mechanisms of RCF damage under such conditions, a novel wet-dry alternation testing method (D/W-A test) was proposed, and rail RCF damage evolution tests were conducted in this study. Detailed comparisons between the novel testing method and three widely used rail RCF methods were analyzed. The results show that under wet-dry alternating conditions, the crack growth rate and wear rate were initially low, with cracks predominantly located in the region near the rail surface. Thus, there was a significant competitive relationship between crack propagation and wear in this period. Then, with the increase in cycling number, RCF damage was gradually dominated by crack propagation, which extended deeper into the material along its deformation orientation. Meanwhile, the severe material spalling led to a rapid increase in wear rate. Through comparative analysis of the accuracy, repeatability, evaluability, rationality, and practicability of the four testing methods, it was found that the novel method proposed in this study had significant advantages in rationality and accuracy compared with traditional RCF testing methods, providing a more effective tool for systematic studies on RCF performance of rail materials.

**Keywords:** rail; rolling contact fatigue; wet-dry alternation; testing method



**Nomenclature**

| | |
|---|---|
| RCF | Rolling contact fatigue |
| SPD | Severe plastic deformation |
| D/W-A | Dry-wet alternation conditions |
| D | Dry condition |
| D-W | Dry followed by wet conditions |
| W | Wet condition |

## 1 Introduction

In recent years, with the high-speed and heavy-load development of railway transportation, the problem of rail rolling contact fatigue (RCF) damage has become increasingly prominent, posing a serious threat to the stability and safety of train operations [1, 2]. Under the continuous action of cyclic contact stress, plastic shear deformation occurs on the rail surface, which in turn leads to the formation of continuous cavities between textures, ultimately resulting in the initiation of RCF cracks [3-6]. Once cracks initiate, the contact stress continues to drive them to propagate along the direction of plastic deformation. Meanwhile, the presence of liquids such as water and oil accelerates the fatigue failure process [7]. From some typical RCF damage characteristics from the cross-section view of rail material as shown in Fig. 1, it can be observed that as the crack depth increases, the angle between the cracks and the rail surface gradually increases, usually ranging from 10° to 40° [8]. Within the plastic deformation zone, crack propagation is influenced by plastic deformation, resulting in fewer branches. However, once the cracks extend beyond this zone, the probability of branching increases significantly. When multiple cracks are interconnected, it leads to surface spalling of the rail [9].

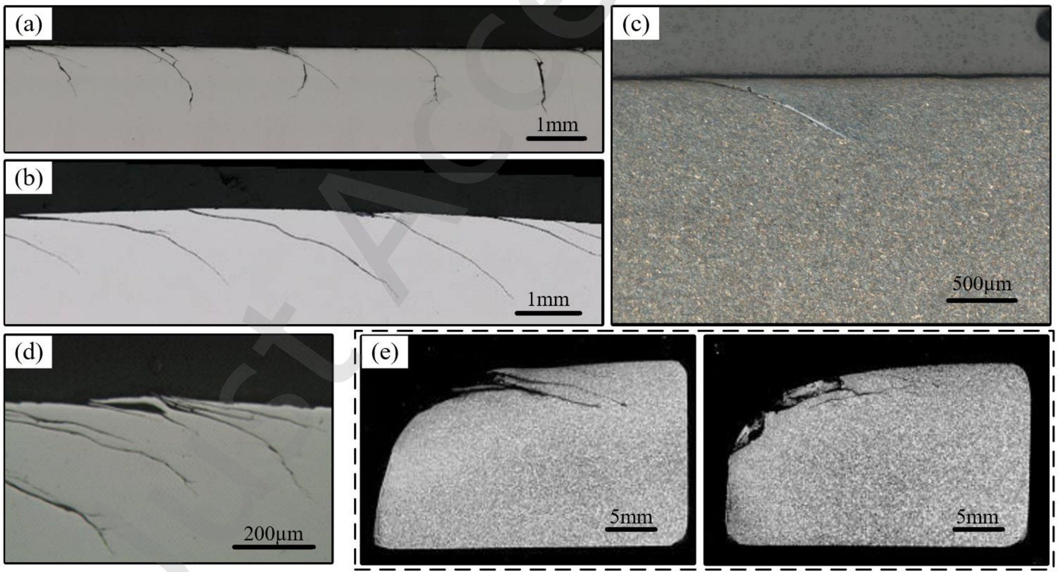


**Fig. 1.** Typical RCF damage in the cross-section of rails: (a) tread cracks in single-track rails; (b) gauge corner cracks in severely side-worn rails [10]; (c) gauge corner cracks in rails without side wear; (d) gauge corner cracks in heavy-duty rails [11]; (e) Gauge corner cracks with peeling damage [12].

Currently, numerous scholars have investigated wheel-rail wear and rolling contact fatigue behavior under dry conditions using a twin-disc rolling testing machine [13-16]. However, the RCF cracks observed in these studies typically exhibit small propagation angles and are mainly confined to the severe plastic deformation (SPD) zone, with limited propagation into the interior of the material [17, 18]. To accelerate crack propagation, wet conditions are often introduced in RCF tests. The fluid entrapment mechanism on crack propagation is shown in Fig. 2. Under dry conditions, the directions of plastic deformation of the wheel-rail samples are opposite to sliding behavior, and cracks initiate and propagate along the deformation direction. When the contact interface is filled with liquid, for the sample for which the plastic deformation direction is the same as the rolling direction, the rolling contact between wheel and rail will first come into contact with the crack opening, thereby leading to the closure of the crack and trapping the liquid inside the crack. Due to the incompressibility of the liquid, the trapped liquid releases compressive stress by propagating the crack when it is squeezed under the continuous wheel-rail cyclic load [19, 20]. Meanwhile, for the other sample which the plastic deformation direction is opposite to the rolling and sliding direction, the rolling contact between wheel and rail will first come into contact with the crack tip, and the liquid inside the cracks will be extruded out, which will not accelerate the crack propagation. Therefore, many researchers, in order to systematically study the RCF damage behavior of wheel-rail systems, first conduct rolling contact tests under dry conditions to prefabricate plastic deformation and initial cracks, and then conduct tests under wet conditions to accelerate crack propagation [5, 21-24]. Also, tests conducted wholly under wet conditions were used to study the RCF lifetime of wheel-rail materials, but these tests typically exhibited a lower degree of plastic deformation and required a longer testing period [25, 26]. However, the actual contact condition of the wheel-rail system is not a continuous dry or wet condition [5, 27]. Rainfall and humidity can cause the wheels and rails to enter a wet condition, and even the rail can undergo multiple transitions from dry to wet conditions within a day [28]. Bodini et al. [29] studied wheel RCF damage under dry-wet conditions using image processing and vibration monitoring systems. However, the alternation period was long, and they failed to explain the RCF damage behavior under such conditions. Therefore, a proper method for an RCF test under dry-wet alternation conditions (D/W-A test) is lacking, and the RCF damage mechanism of the rail under these conditions remains unexplained.

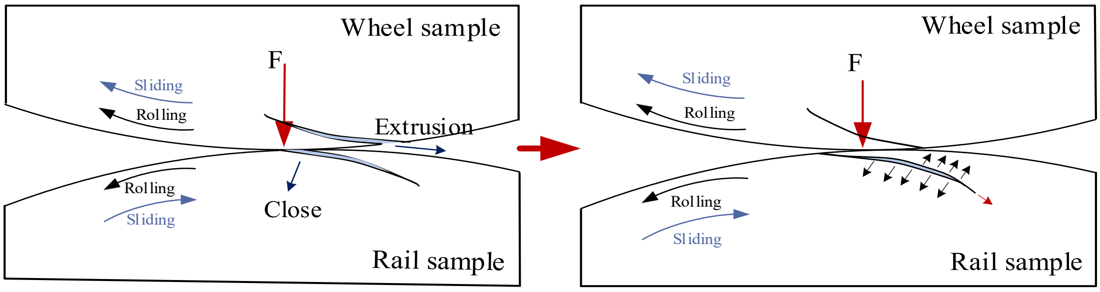


**Fig. 2.** Schematic diagrams of the fluid entrapment mechanism.

## 2 Experimental details

This study was conducted on the MJP rolling contact wear and fatigue testing machine, as shown in Fig. 3 [30]. The rotation of the two shafts was driven by two servo motors. Servo motor 1 was connected to the shaft where the rail sample was installed via two synchronous belts. Servo motor 7 was connected to the wheel sample via a torque sensor. The shaft on the bearing block was connected to the load transfer arm and the synchronous belt. The normal load between the wheel-rail sample was realized by the hydraulic cylinder rod through the load transfer arm.

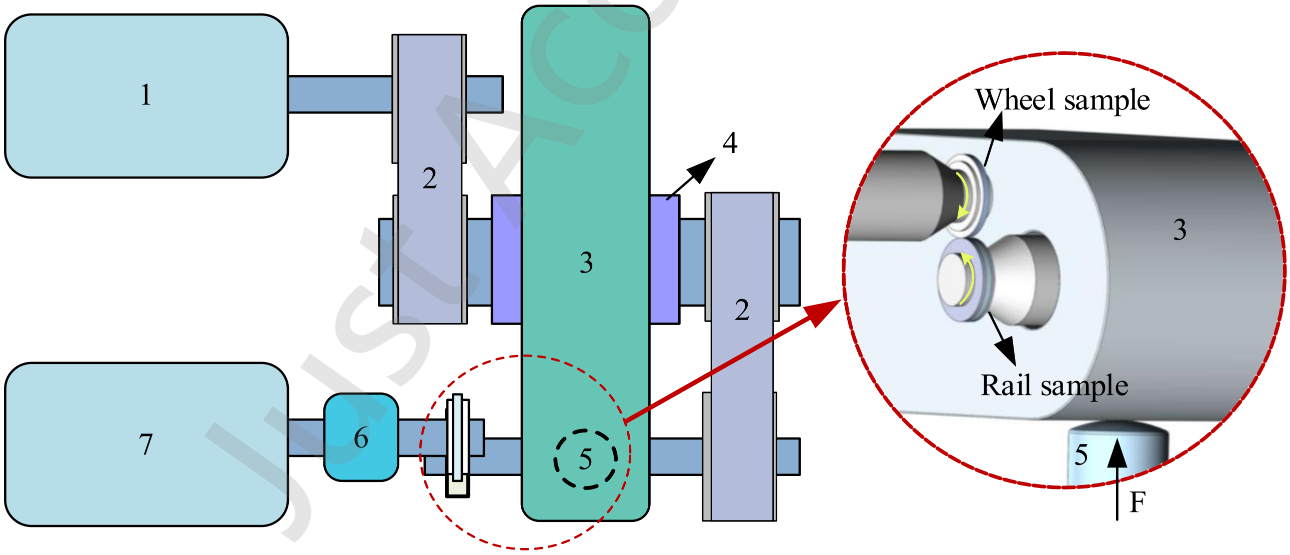


**Fig. 3.** The schematic diagram of the MJP rolling contact wear and fatigue testing machine: 1, 7. Servo motors; 2. Synchronous belt; 3. Load transfer arm; 4. Bearing block; 5. Hydraulic cylinder rod; 6. Torque sensor.

Testing methods used in this study are shown in Fig. 4, while the testing parameters are listed in Table 1. Tests 1-4 were aimed at exploring an optimized testing method that could accurately and stably simulate the typical RCF damage as shown in Fig. 1 (i.e., as the crack depth increases, the angle between the cracks and the rail surface gradually increases). Thus, the adjustment of the contact parameters (rotational speed, vertical force, and slip ratio), dry-wet alternating methods (duration of wet condition), and running-in tests were included in tests 1-4. The reasons for the adjustments were explained in detail in the following section, in conjunction with the testing results.

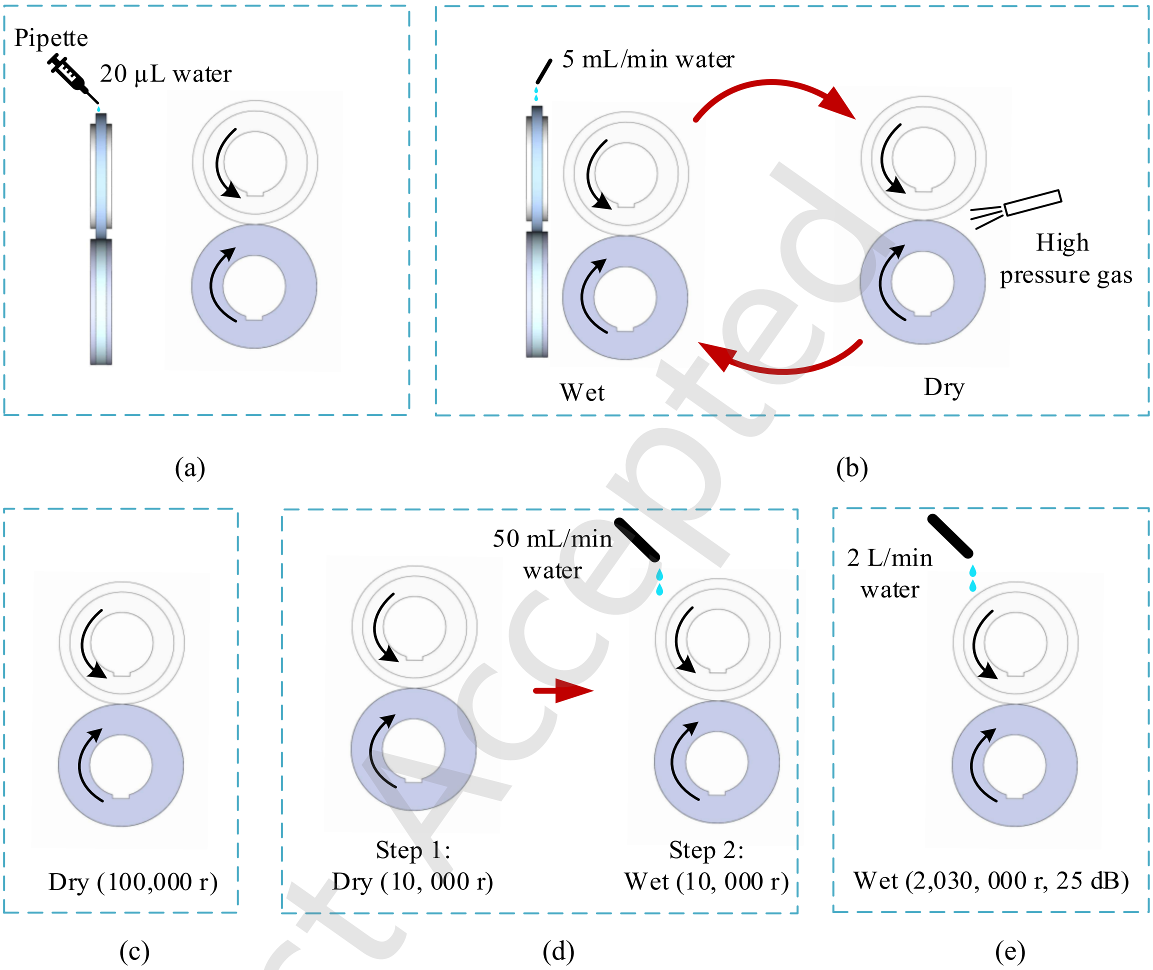


**Fig. 4.** The process of different testing methods, (a) dry-wet alternation method 1; (b) dry-wet alternation method 2; (c) test 8; (d) test 9; (e) test 10.



Two kinds of dry-wet alternation methods are shown in Figs. 4a and b. As for the dry-wet alternation method 1 (tests 1-2), the application of 20 μL water into the wheel-rail interface was realized by a pipette every 30 seconds (20 μL/30 s) (Fig. 4a), regardless of whether the wheel-rail contact surface recovered to a dry condition after 30 s. The procedure of the dry-wet alternation method 2 (tests 3-4) is illustrated in Fig. 4b. During the wet condition, a peristaltic pump was used to apply water medium into the wheel-rail interface at a flow rate of 5 mL/min, ensuring an adequate supply of water at the interface. When transitioning from wet to dry conditions, the flow pump was turned off, and high-pressure air was blown onto the wheel-rail interface to realize the restoring dry contact rapidly. Thus, by connecting the flow pump and the air pressure valve through a timed cycling controller, the automation of dry-wet alternation was achieved. Mentioned that the duration of the wet condition would have an impact on the results, as the water medium would accelerate crack propagation. Also, the rotational speed, the vertical force, and the slip ratio in test 1 were 500 rpm, 2,750 N (contact stress of 1,150 MPa), and 1 %, respectively [31]. Among them, a contact stress of 1150 MPa was adopted to simulate an axle load of 21 t, while a slip ratio of 1% was commonly used in wheel-rail contact test investigations [32, 33]. Subsequently, the vertical load (Test 2) and the slip ratio (Test 4) were reduced to 1,300 N (corresponding to a contact stress of 800 MPa) and 0.6%, respectively, with the aim of reducing the wear at the wheel-rail interface by lowering the tangential force [34]. In this way, due to the competitive relationship between wear and RCF behavior, RCF crack propagation behavior could be amplified. Furthermore, to ensure stability during the initial stages of the test, a running-in test of 10,000 cycles under dry conditions before conducting the wet-dry alternation testing process was considered to improve the testing method.

Based on the result that the characteristics of rail damage observed in test 4 were similar to the typical rail RCF damage (Fig. 1), the dry-wet alternation testing method after a 10,000 cycles running-in test was chosen as the optimized testing method. The rotational speed, the vertical force, and the slip ratio were 500 rpm, 1,300 N, and 0.6 %, respectively. Thus, tests 5-7 were conducted to study the evolution of rail damage based on the optimized testing method. After a running-in test of 10,000 cycles, the durations of tests 5-7 were 30,000, 60,000, and 100,000 cycles (i.e., 30, 60, and 100 cycles of 60 s dry/60 s wet), respectively.

**Table 1** Testing parameters

| Test number | Test speed(rpm) | Vertical load(N) | Slip ratio (%) | Dry/Wet | Running-in test number of cycles (r) | Formal test number of cycles (r) |
|---|---|---|---|---|---|---|
| 1 | 500 | 2,750 | 1 | 20μL water/30 s | 0 | 20,000 |
| 2 | | 1,300 | 1 | 20μL water/30 s | 0 | 20,000 |
| 3 | | 1,300 | 1 | 40 s Dry/20 s Wet | 0 | 20,000 |
| 4 | | 1,300 | 0.6 | 60 s Dry/60 s Wet | 10,000 | 10,000 |

| | | | | | | |
|---|---|---|---|---|---|---|
| 5 | | 1,300 | 0.6 | 60 s Dry/60 s Wet | 10,000 | 30,000 |
| 6 | | 1,300 | 0.6 | 60 s Dry/60 s Wet | 10,000 | 60,000 |
| 7 | | 1,300 | 0.6 | 60 s Dry/60 s Wet | 10,000 | 100,000 |
| 8 | 500 | 2,750 | 1 | Dry | 0 | 100,000 |
| 9 | 500 | 2,750 | 1 | Wet | 10,000 | 10,000 |
| 10 | 1,500 | 2,750 | 1 | Wet | 0 | 2,030,000 |

Three typical RCF tests (Test 8-10) were used to compare and evaluate the D/W-A RCF test and the existing RCF testing methods. Test 8 was performed under dry condition (D test), as shown in Fig. 4c. Test 9 initially performed 10,000 cycles under dry conditions, followed by 10,000 cycles under wet conditions, constituting the dry-wet test (D-W test), as illustrated in Fig. 4d. Test 10 was conducted entirely under wet condition (W test), the test stopped when the vibration amplitude of wheel-rail system exceeded 25 dB based on the failure criterion, at this time, the test was running for 2,030,000 cycles. It is worth noting that the D, D-W, and W test methods exhibited a significant difference in principle. Therefore, the same cycling number cannot be applied, as this would fail to achieve the intended purpose of the RCF tests.

After the completion of the tests, the wheel-rail samples were soaked in anhydrous ethanol and cleaned using ultrasonic waves. Following the drying process, the samples were precisely weighed on an electronic balance (JA4103, China) with an accuracy of ±0.1 mg. The wear amount of the rail was then determined by the mass difference before and after the test. The surface damage of the rail was observed and analyzed using an optical microscope (OM, KEYENCE VHX-6000, Japan). As depicted in Fig. 5, the rail samples were dissected using wire cut electrical discharge machining. The cross-sectional samples were then mounted using a metallographic mosaic [18]. After undergoing mechanical grinding and polishing, the polished cross-sections were etched using a 4 % nitric acid in alcohol solution to reveal the microstructure. The plastic deformation of the rail was then observed and analyzed using OM, while the crack propagation and microstructure evolution were examined using a scanning electron microscope (SEM, Phenom Pro-SE, Netherlands). For the rail samples from the D/W-A test, the methods for measuring crack depth, width, and length are shown in Fig. 6.

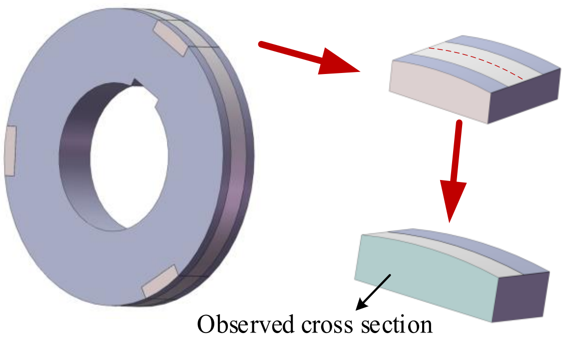


**Fig. 5.** Sampling position of cross-sectional samples.

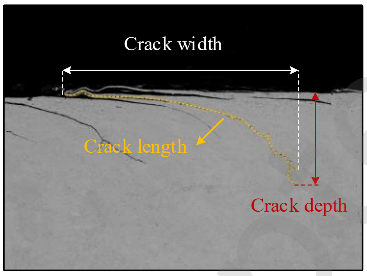


**Fig. 6.** Measuring method of crack characteristics.

## 3 Result

The comparison of various dry-wet alternation testing processes in tests 1-4 is first discussed in this section, and an optimal procedure is determined to be used in tests 5-7. Then, the evolution of damage under dry-wet alternation conditions is discussed. Also, the comparison of RCF tests using different methods is included to evaluate the RCF testing methods.

### 3.1 Exploration of testing methods for dry-wet alternation conditions

In tests 1-4, by analyzing the adhesion coefficient, wear, damage behavior, and RCF cracks characteristics as shown in Figs. 7-10, it was verified whether the tests could accurately and stably simulate typical RCF damage (Fig. 1). Based on these damage behaviors, the contact parameters, wet-dry alternating methods, and running-in tests were further adjusted to explore the optimized D/W-A test parameters.

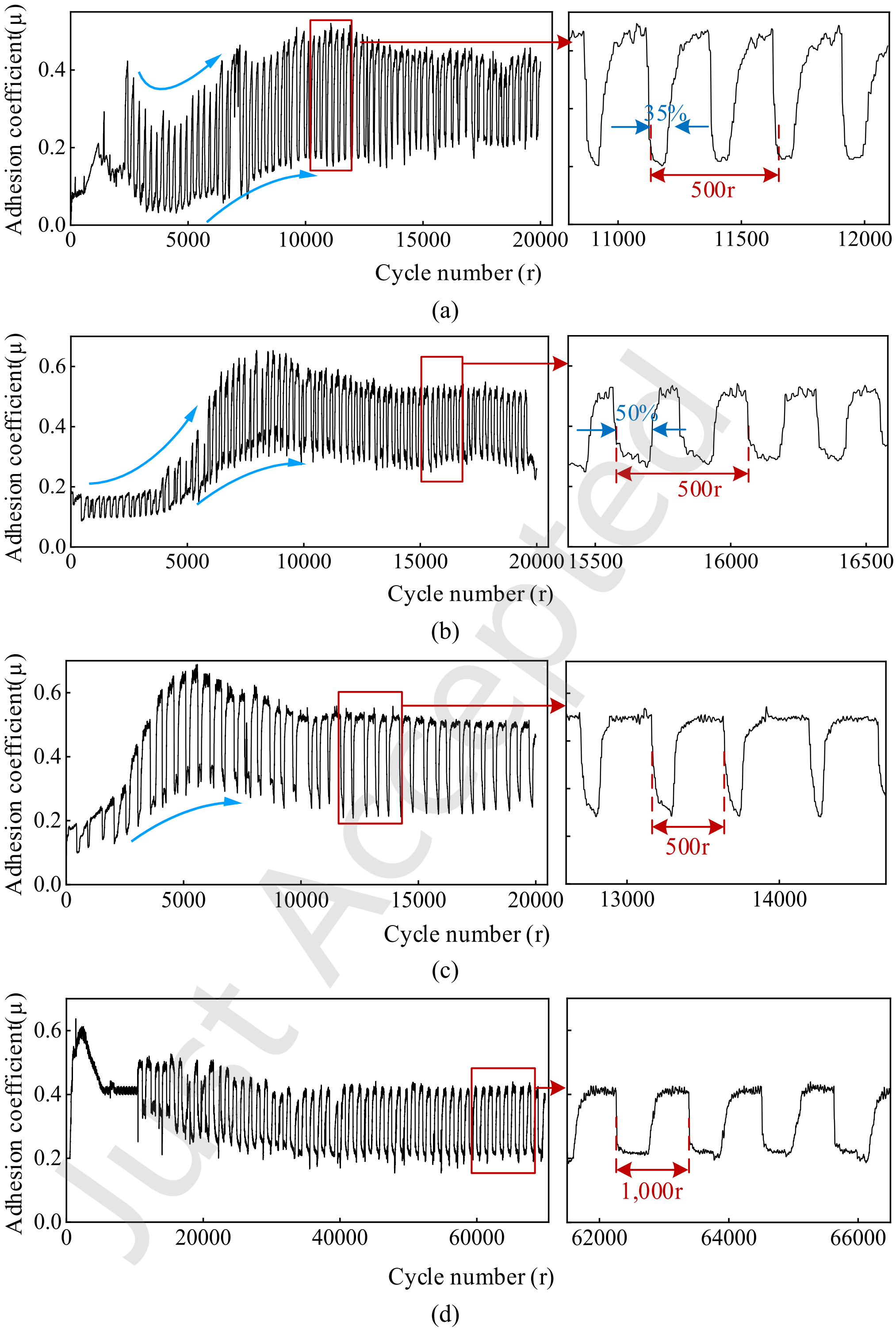


**Fig. 7.** Adhesion coefficient of different dry-wet alternation methods: (a) test 1; (b) test 2; (c) test 3; (d) test 6.

It can be indicated from Fig. 7a that after each interval of water application in test 1, the adhesion coefficient rapidly decreased and remained stable for a certain period, subsequently increased gradually due to the depletion of water. Additionally, the low adhesion coefficient condition (i.e., wet condition) accounted for approximately 35 % of the dry-wet alternation cycles.

As shown in Fig. 8, test 1 had a rail wear amount of 0.18 g, with a relatively high wear rate (48.5 μg/m). A high level of wear indicated that RCF cracks were more prone to be removed, due to the competition between rail wear and RCF [35, 36]. Cracks were spread over the rail surface and accompanied by a large amount of black oxides (Fig. 9a) [37]. As for the depth of the plastic deformation layer, it was evident that the plastic deformation in test 1 was the most significant. Severe plastic deformation was accompanied by a high crack initiation rate, but also by a higher wear rate. As presented in Fig. 10, it should be noted that in test 1, while the crack length and depth were large, the ratio of crack depth to length was small. So, the cracks remarkably propagated along the surface and not inwardly into the matrix along the plastic deformation orientation, which is different from the typical rail crack morphology in Fig. 1.

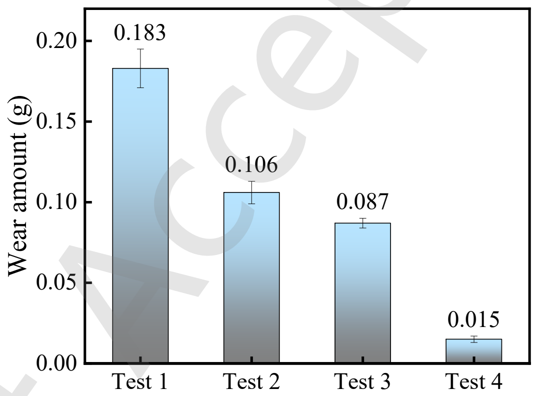


**Fig. 8.** Rail wear amount of different dry-wet alternation methods.

Therefore, in order to further amplify crack propagation behavior by reducing wear action (the competitive relationship between wear and RCF), the contact stress in test 2 was reduced from 1,150 MPa to 800 MPa to reduce the wear action. Based on the observation of rail wear amount, damage behavior, and crack characteristics presented in Figs. 8, 9b, and 10, it was evident that despite a reduction in wear amount, the cracks did not propagate further into the material. Meanwhile, due to the reduction of the contact stress, the depletion rate of water at the wheel-rail interface slowed down. This resulted in an increase in the duration where a lower adhesion coefficient was observed, accounting for 50 % of the alternation cycle. It was evident that when using the dry-wet alternation method 1 (20 μL/30 s), the time for the wheel-rail interface to resume a dry condition could not be guaranteed. Therefore, to conduct the test with greater precision, a peristaltic pump was used for quantitative control of the testing durations in wet conditions (Fig. 4b, the dry-wet alternation method 2) in tests 3 and 4.

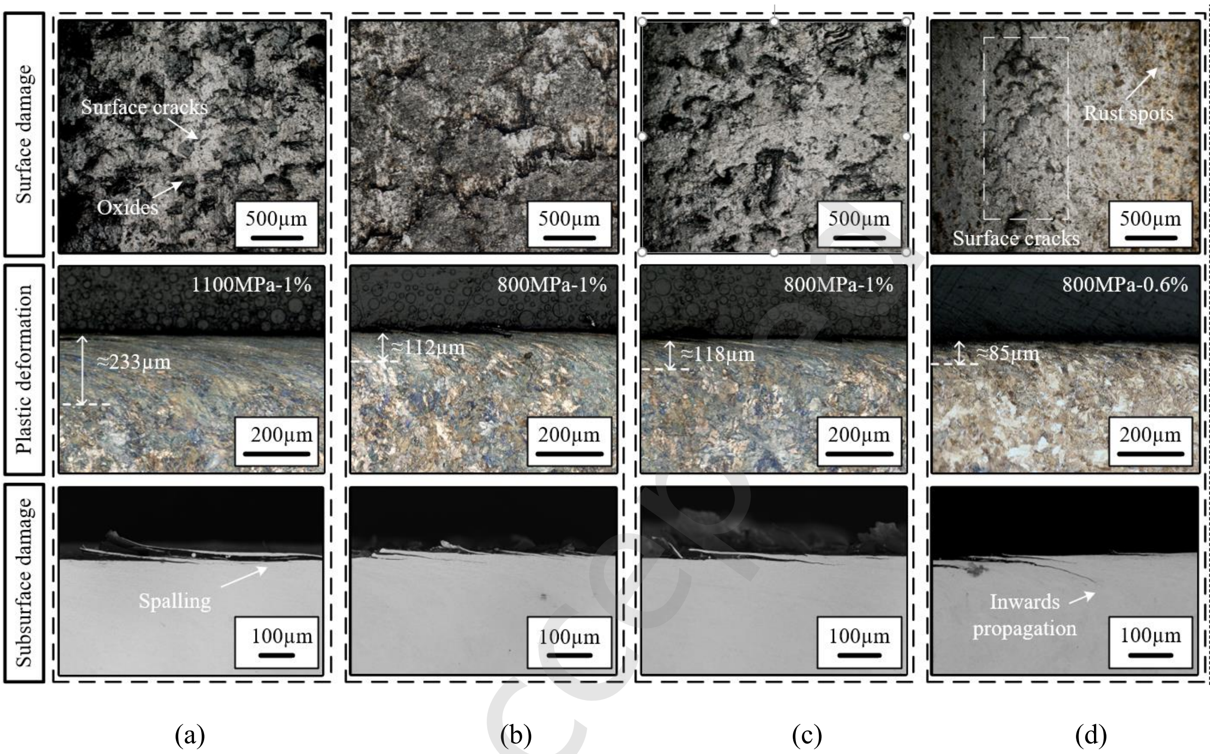


**Fig. 9.** Damage behavior of rails of different dry-wet alternation methods: (a) test 1; (b) test 2; (c) test 3; (d) test 4.

In the test 3, compared to the test 2, although the rail wear was lower and the ratio of crack depth to length was also reduced, the damage characteristics still did not align with typical rail RCF damage (Fig. 1). Then, it can be seen in Fig. 7, in tests 1-3, with the cycling number increasing, the adhesion coefficient gradually increased, reached a certain level before slightly decreasing, and finally stabilized. The phenomenon was mainly attributed to the smooth surface of the wheel and rail samples before the test, as well as the inevitable installation error. However, as the test progressed, the contact interface stabilized, and the period from the beginning of the test to the stable contact state of the wheel-rail interface is called the running-in test. It was worth noting that the running-in process exhibited instability under dry-wet alternation conditions. Consequently, in the subsequent tests 4, a running-in test of 10,000 cycles was conducted under dry conditions before the tests were carried out under dry-wet alternation conditions.

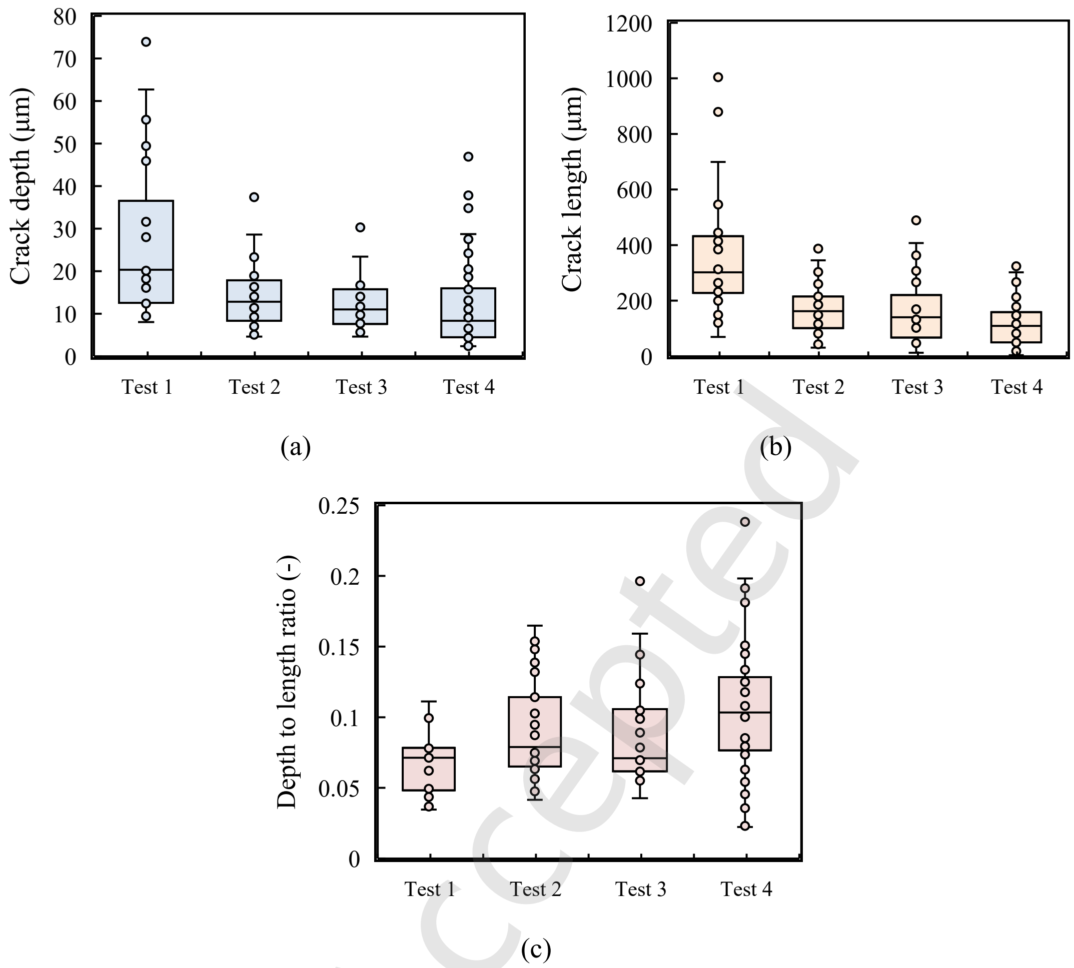


**Fig. 10.** RCF cracks characteristics of tests 1-4: (a) crack depth, (b) crack width, (c) depth to length ratio.

Also in test 4, because the contact stress of 800 MPa is approximately the minimum value in the railway operation, the slip ratio was further reduced from 1 % to 0.6 % to decrease the rail wear. At the same time, the duration of wet condition was increased from 20 seconds to 60 seconds (60 s Dry/60 s Wet), aiming to accelerate the propagation of cracks. As demonstrated in Fig. 9d, only a certain area of the rail surface exhibited cracks, while the unaffected areas displayed yellowish-brown rust spots. The most interesting finding was that cracks propagated inwardly into the matrix along the plastic deformation orientation. Based on the characteristics of RCF cracks in tests 1-4, it should be noted that although the rail crack length and depth in test 4 were the smallest, the ratio of crack depth to length was maximal (Fig. 10). This indicated that cracks were more likely to propagate deeper into the material. Ultimately, the characteristics of rail damage observed in test 4 were similar to the typical rail RCF damage (Fig. 1).

### 3.2 Evolution of damage under dry-wet alternation conditions

It can be seen from Fig. 11 that the rail wear amount increased with the increase in the cycling number, but this increase was not linear. During the first 10,000 cycles, the rail exhibited a low wear rate. Subsequently, the wear rate began to increase, stabilizing between 30,000 cycles and 60,000 cycles. However, when the test was run after 100,000 cycles, the wear rate rapidly increased, indicating severe wear conditions [35].

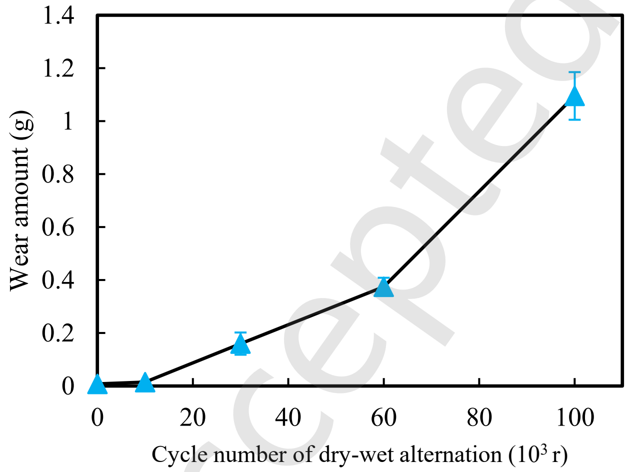


**Fig. 11.** Rails wear amount with various cycling numbers.

The damage evolution in the rail is indicated in Fig. 12. It was observed that the surface of the rail was riddled with dense cracks, accompanied by spalling. Based on the morphologies from a cross-sectional view, it was evident that the plastic deformation layer depth gradually increased as the test continued. Additionally, the RCF cracks steadily propagated deeper into the material, with some cracks exhibiting a "C" shape at 100,000 cycles. The crack characteristics are displayed in Fig. 13. With the increase in the cycling number, the depth, width, and length of the cracks also steadily increased. Meanwhile, the crack density slightly decreased from 6 cracks/mm to 5 cracks/mm. This stable evolution of RCF crack characteristics indicated the controllability of the D/W-A testing method.

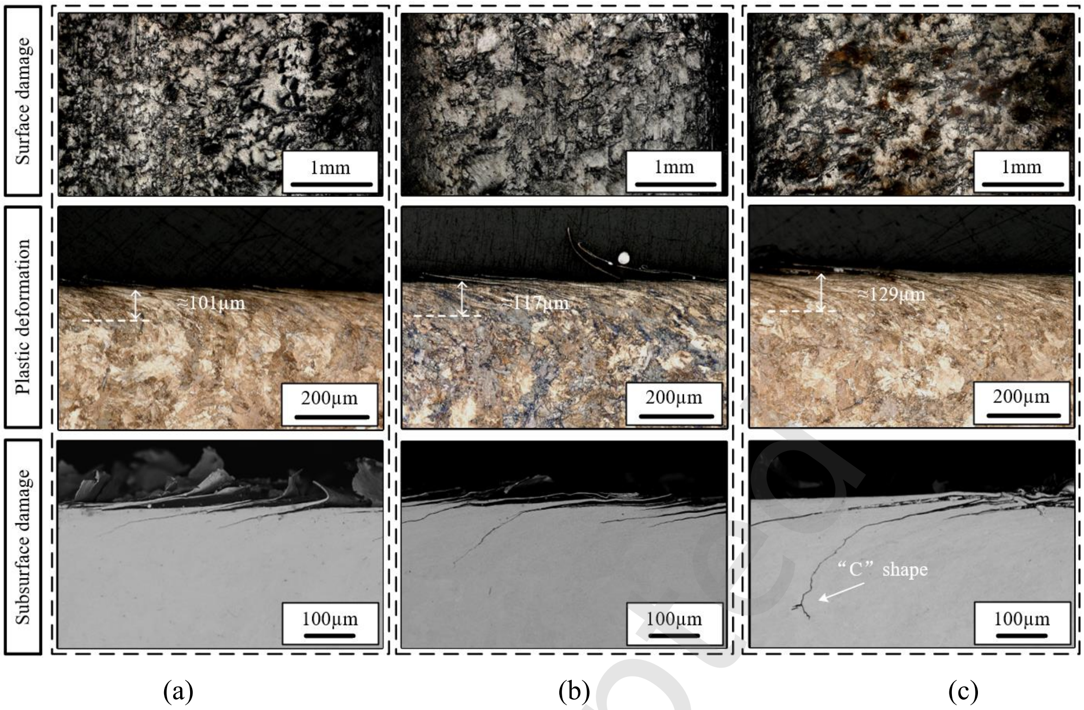


**Fig. 12.** Damage behavior of rails of different cycle numbers under dry-wet alternation: (a) 30,000 cycles; (b) 60,000 cycles; (c) 100,000 cycles.

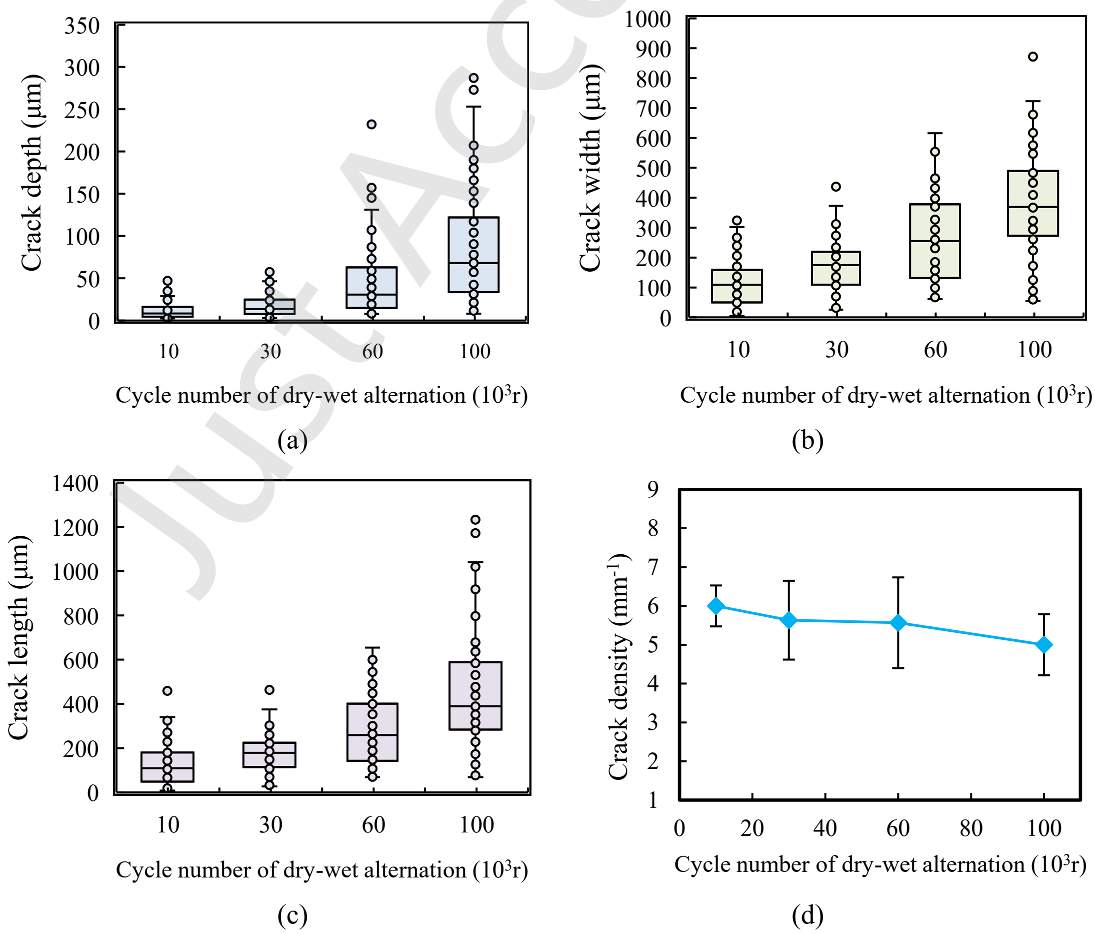


**Fig. 13.** RCF cracks characteristics of different cycle numbers: (a) crack depth; (b) crack width; (c) crack length; (d) crack density.

### 3.3 Comparison of RCF tests using different methods

The adhesion coefficient using various RCF testing methods is shown in Fig. 14. In the D RCF test conducted under dry condition, the adhesion coefficient initially exhibited a rapid increase, followed by a slight decrease, eventually stabilized at approximately 0.3 (Fig. 14a). In the D-W test, the adhesion coefficient rapidly decreased from 0.4 to 0.15 after the application of water medium (Fig. 14b). In the W RCF test, the adhesion coefficient was consistently maintained below 0.1. This was attributed to the lubrication effect of water and the original smooth surface of the wheel-rail sample. Consequently, the wear rate was slow, resulting in an extended running-in period. So, before reaching 400,000 cycles, the adhesion coefficient displayed significant fluctuations before gradually increasing. Following this, during the following 1,200,000 cycles, the adhesion coefficient exhibited another period of fluctuation before gradually declining towards the conclusion of the test.

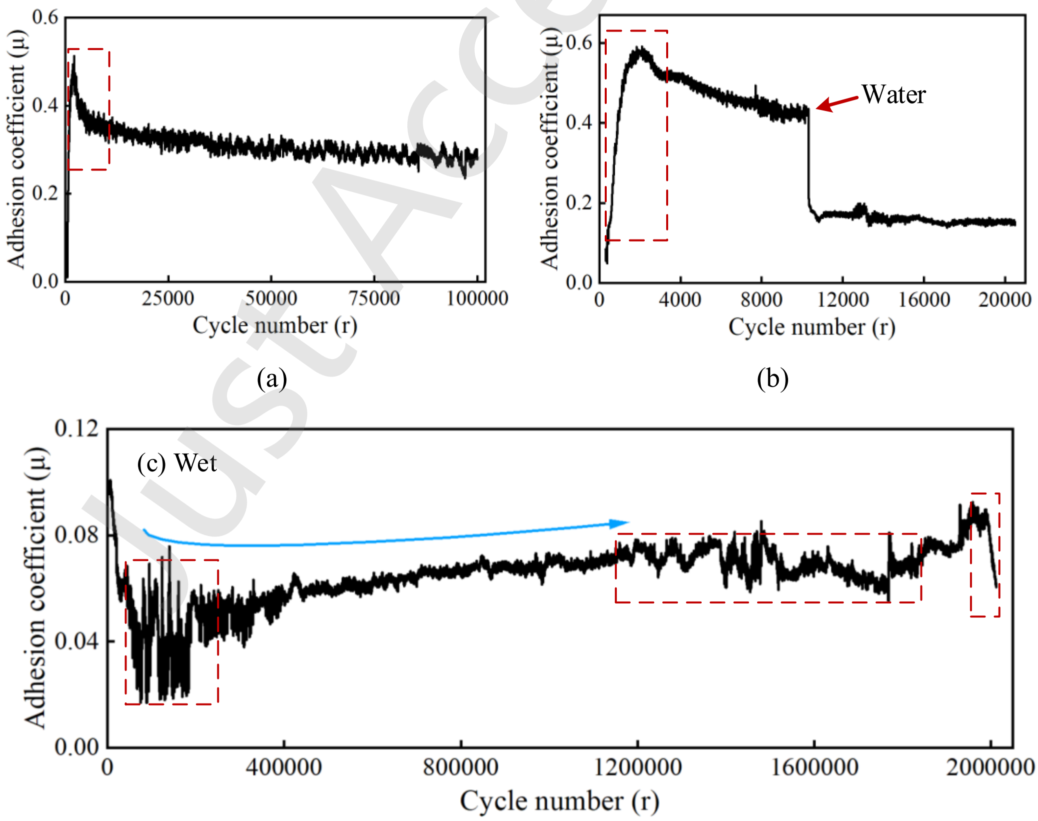


(c)

**Fig. 14.** Adhesion coefficient of RCF test using different methods: (a) D RCF test; (b) D-W RCF test; (c) W RCF test.

Fig. 15 displays the damage behavior in the rail of three kinds of RCF tests. It could be indicated that the mildest RCF damage occurred during the D RCF test, while the crack depths and angles were small. Then, in the D-W RCF test, the surface cracks appeared in a flake-like pattern, with severe spalling. The thickness of the plastic deformation layer was significantly lower compared to the D RCF test due to the less deformation under water conditions and the continuous material spalling. Merely after running for 10,000 cycles under water conditions, the crack depth exceeded 300 μm, taking on a "C" shape and started to branch. This indicated that when using the D-W testing method, crack propagation was extremely rapid, making it difficult to capture the crack growth at different stages. Besides, the most severe RCF damage occurred in the W RCF test because the test terminates upon severe spalling. Spalling pits with a width of 3 mm could be observed from the surface view, while a dense network of cracks could be seen from the cross-section view, with the minimum plastic deformation, with a depth of approximately 10 μm.

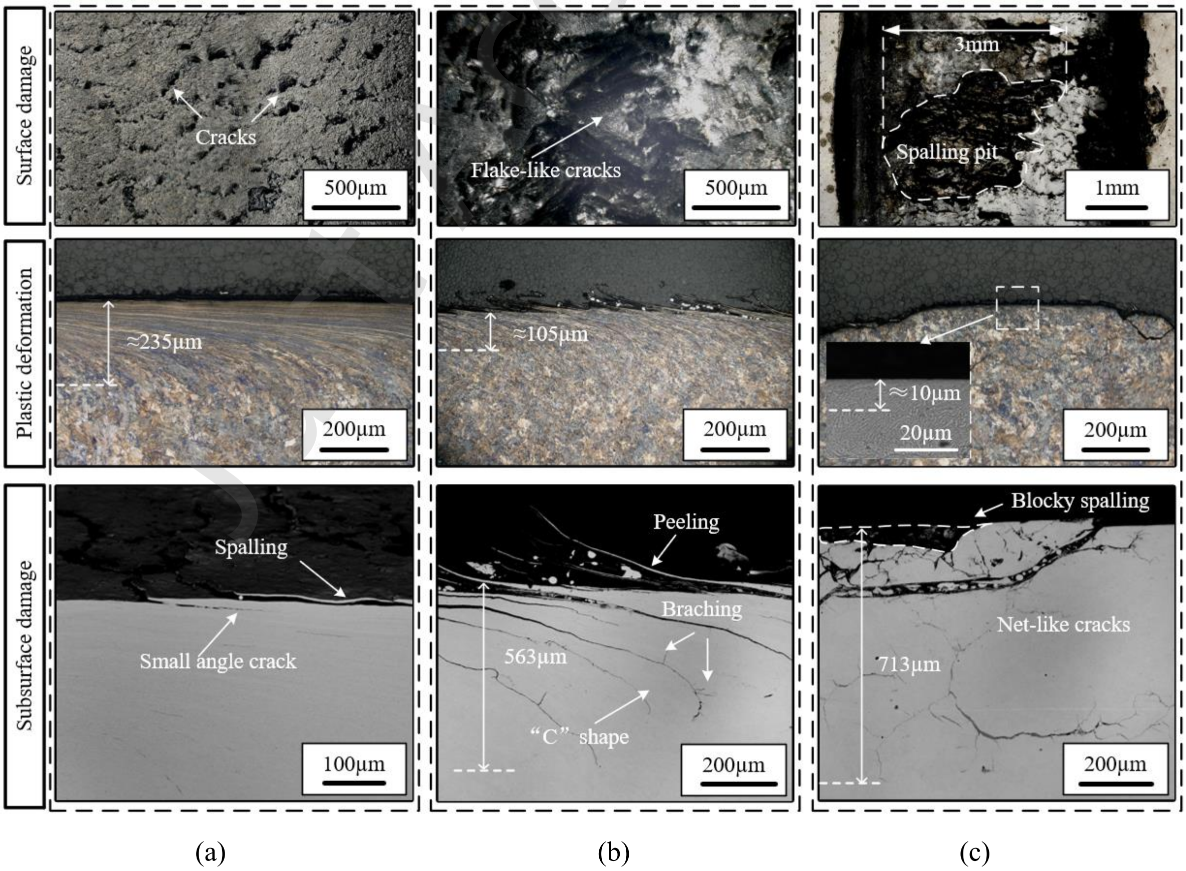


**Fig. 15.** Damage behavior of the rail of RCF test using different methods: (a) D RCF test; (b) D-W RCF test; (c) W RCF test.

## 4 Discussion

### 4.1 Damage mechanism of rails under dry-wet alternation conditions

To further understand the evolution of rail RCF damage behavior under dry-wet alternation conditions, the damage mechanisms were discussed in three stages: the running-in test, the initial period of the dry-wet alternation test, and the later period of the dry-wet alternation test. This discussion was carried out in conjunction with previously revealed damage mechanisms in previous studies under dry and wet conditions, as illustrated in Fig. 16.

As mentioned above, the running-in test was primarily designed to take advantage of the higher wear rate under dry conditions, allowing the wheel-rail interface to quickly reach a stable contact state [38], which can improve the repeatability of the D/W-A test. Under this stage, plastic deformation accumulated and cracks initiated in the rail materials due to the ratcheting effect [35]. The RCF cracks initiated during this period were mainly characterized by small angles and typically do not propagate deep into the material due to the lack of sufficient driving force for crack propagation [3]. Then, in the initial period of dry-wet alternation, crack propagation was not significantly accelerated by the fluid entrapment mechanism (Figs. 12 and 13). Although the fluid entrapment mechanism was already operative once water infiltrated the cracks, its effect remained limited at this stage. This was mainly because only a small amount of water was able to enter the small cracks initiated during the running-in period, resulting in a relatively low crack driving force induced by the fluid entrapment mechanism under wet conditions [33]. When the wheel-rail interface transitioned to dry conditions, the wear action would increase due to the increase in adhesion coefficient (Fig. 7). Some surface cracks were removed by wear due to the competitive relationship between wear and RCF damage [35, 39]. Meanwhile, plastic deformation and crack initiation also occurred on the rail surface during the dry phases of the dry-wet alternation cycles. Then, with the continuous short-term alternation of dry and wet conditions at the wheel-rail interface, an interesting phenomenon the distribution and propagation of cracks were not uniform, as shown in Fig. 9d. This was because individual cracks often propagated faster than others. These cracks were typically initially aided by liquid compression force, resulting in rapid propagation in certain areas, as illustrated in Fig. 9d. Cracks not only propagated into the material but also along the surface. After a certain number of cycles, the cracks would eventually fill the entire contact area, as shown in Fig. 12a.

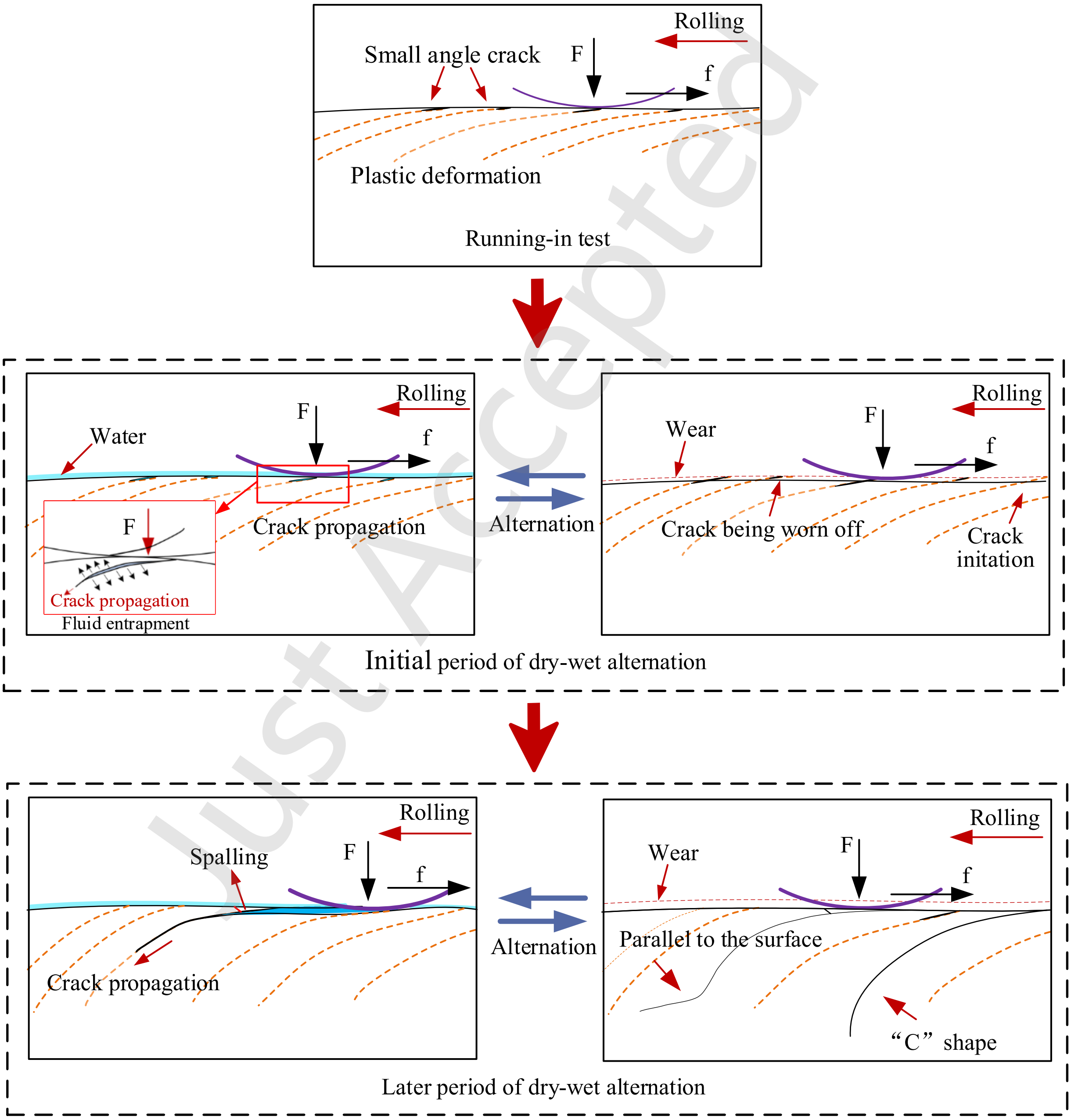


**Fig. 16.** Schematic of RCF damage in the rail under dry-wet alternation conditions.

Finally, in the later period of wet-dry alternation, some cracks exhibited an increasing tendency to propagate into the material interior (Fig. 13). This crack morphology allowed water to become more easily trapped within the cracks, enhancing the fluid entrapment and leading to an accelerated crack propagation rate. The rail also experienced severe fatigue wear due to crack spalling [40], resulting in a rapid increase in wear during this period (Fig. 11). After transitioning to a dry condition, the dominant damage mode shifted to wear, and the surface cracks were worn off first. The initiation of cracks and material deformation was always present, but as the depth and length of cracks increased, contact stress could penetrate deeper through the cracks, leading to more severe deformation (Fig. 12). Additionally, an interesting phenomenon under dry-wet alternation conditions was that the crack was not prone to branching (Fig. 12c). This was because, in the deformation region, cracks tend to propagate along the path orientation with the least resistance, resulting in less crack branching [4, 41].

In summary, under dry-wet alternation conditions, the propagation rate of rail RCF cracks exhibited a trend of slow growth followed by acceleration, accompanied by continuous wear and plastic deformation. This dynamic coupling of crack propagation, wear, and plastic deformation more accurately simulated the damage behavior of rails during actual service. Moreover, under dry-wet conditions, the continuous propagation of RCF cracks further exacerbated rail wear. This indicated that in regions with rainy and humid conditions (i.e., under dry-wet alternation conditions), rails were not only prone to severe RCF damage but also experienced accelerated wear due to intensive spalling.

### 4.2 Evaluation of RCF testing methods

This study exclusively conducted W, D-W, and W tests under single-parameter conditions, aiming to compare the three testing methods and the D/W-A test using unified experimental equipment, materials, and analytical methods. It should be noted that these three testing methods have been widely employed in the field of wheel-rail rolling contact fatigue research. To systematically evaluate the differences among the four RCF test methods, Table 2 specifically compiles the typical wheel-rail RCF damage characteristics observed in studies that used these three testing methods. Additionally, the forms of rail crack morphologies that resulted from the four RCF testing methods are displayed in Fig. 17.

The D RCF testing method was typically used to study the rolling wear and crack initiation behavior of wheel-rail materials. Under dry condition, crack propagation was primarily concentrated in the SPD region, exhibiting small-angle, long, and straight crack characteristics (Fig. 17a). Based on the data in Table 2, the crack depth was generally less than 30 mm and much smaller than the crack length, which was significantly different from the typical RCF damage morphology (Fig.1) [42]. This was mainly attributed to the fact that, under dry conditions, although the wheel-rail materials experienced a high rate of crack initiation due to the ratcheting effect, the driving force for cracks to propagate into the deeper layers was insufficient. Meanwhile, the high wear rate of materials under dry conditions led to a significant competition between wear and RCF [35, 39]. This competitive mechanism made the shallow cracks more easily removed by wear, reducing the correlation between crack size and test parameters or material properties, thereby affecting the comparative evaluation of the RCF damage performance of wheel-rail materials [3, 43].

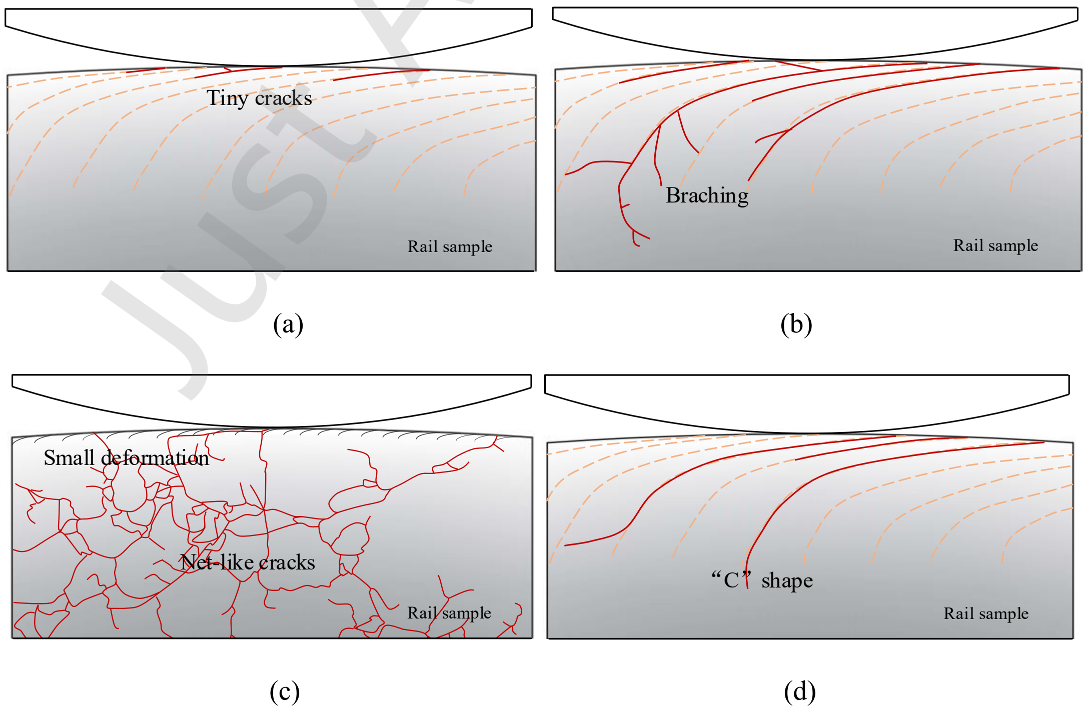


**Fig. 17**. Schematic diagrams of crack profiles in the rail resulting from different RCF testing methods: (a) D test; (b) D-W test;(c) W test; (d) D/W-A test.

**Table 2** RCF damage characteristics using different RCF test methods

| Test Method | Reference | • Contact stress<br>• Speed<br>• Slip ratio<br>• Cycling number<br>• Materials | Cycle number/ $10^3$ cycles | RCF damage characteristics |
|---|---|---|---|---|
| D test | [42] | • 1230 MPa<br>• 500 rpm<br>• 0.5 %<br>• 3 types of wheel materials | • 5~400 | • Crack depth: 0 μm~24.5 μm<br>• Crack length: 0 μm~410 μm<br>• Crack depth and length increase rapidly at first, then gradually with the cycle number |
| | [3] | • 850 MPa<br>• 200 rpm<br>• 0.17 %~9.43 %<br>• 3 types of wheel materials | • 180 | • Crack depth: 8.1 μm~28.9 μm<br>• Crack length: 65 μm~295 μm<br>• Crack angle: 2.8°~11.6°<br>• The influences of the creepage and materials on the depth and length of cracks are not clear |
| | [35] | • 1,161 MPa;<br>• 500 rpm<br>• 0.5 %~5 %<br>• 3 types of rail materials | • 100 | • Crack depth: 4.6 μm~28.7 μm<br>• Crack length: 58.5 μm~327 μm<br>• Crack angle: 3.8°~9.2° |
| D-W test | [33] | • 1,100 MPa<br>• 500 rpm<br>• 1 %<br>• U71Mn | • Dry: 15<br>Wet: 5~50 | • Crack depth: 27.6 μm~364 μm<br>• Crack length: 256 μm~1036 μm |
| | | | • Dry: 5~50<br>Wet: 15 | • Crack depth: 105 μm~423 μm<br>• Crack length: 589 μm~2056 μm |
| | [44] | • 1131 MPa<br>• 500 rpm<br>• 1 %<br>• Different wheel-rail materials match | • Dry: 10<br>Wet: 20 | • Crack depth: 185 μm~400 μm<br>• Crack length: 500 μm~1900 μm<br>• As the material hardness increased, the crack depth and length decreased |
| W test | [45] | • 1,450 MPa<br>• 1,440 rpm<br>• 0.5 %<br>• Different wheel materials | • 100<br>• 200<br>• 300<br>• 400<br>• 550 | • At $3\times10^5$ cycles, no surface RCF cracks appeared<br>• At $4\times10^5$ cycles, the RCF surface cracks were produced<br>• At $5.5\times10^5$ cycles, the bulk spalls (＞3 $mm^2$) occurred to cause the RCF failure |
| | [46] | • 1,230 MPa<br>• 1,500 rpm<br>• 0.3 %<br>• D2 wheel materials | • 514~2,583 | • The area of shelling ranged from 2 to 12 $mm^2$ without significant regularity<br>• Shelling and Net-like RCF subsurface cracks |

The D-W RCF testing method was the most widely used approach for experimental studies of crack propagation in wheel-rail materials. Cracks initiated under dry conditions and subsequently propagated under wet conditions with the aid of the fluid entrapment mechanism. This method effectively overcame the technical bottleneck of crack propagation in dry conditions while also offering the advantage of a short test duration, thus demonstrating outstanding practical value within the current wheel-rail RCF testing system. However, the D-W test method still had several limitations. Firstly, the fully wet crack propagation mode differed significantly from the predominantly dry contact service conditions of actual wheel-rail contact. Moreover, the low shear stress environment under wet conditions suppressed the accumulation of plastic deformation, resulting in the gradual thinning of the plastic deformation layer due to the spalling of surface cracks and the formation of a network of propagating cracks in the matrix region (Fig. 17b) [40]. Secondly, the crack propagation rate under wet conditions was excessively high, with a crack depth of 423 μm developing after only 15,000 cycles (Table 2) [33]. Although this high propagation rate significantly reduced the test duration, it hindered the complete observation of the damage evolution process. Thirdly, the crack initiation under the initial dry conditions significantly interfered with the propagation behavior under the following wet conditions. In particular, the early dry contact of the test often experienced running-in conditions with considerable fluctuations in crack initiation, which further amplified the system error.

The W RCF test method was a standardized method widely used in the bearing and gear industries to evaluate the rolling contact fatigue (RCF) life of metallic materials under lubricated conditions. This test was typically terminated based on a fatigue failure criterion, such as when the spall area exceeded a threshold of 3 $mm^2$. The number of cycles corresponding to this failure point was defined as the RCF life. The testing duration can extend up to $1\times10^7$ cycles, resulting in significant costs [47]. In addition, due to the suppressive effect of full lubrication on the ratcheting mechanism, the initiation rate of surface cracks was substantially reduced. As shown in Table 2, surface cracking was observed only after 400,000 cycles [45]. It was noteworthy that, upon termination of the W test (i.e., at RCF failure), the subsurface morphologies of material typically exhibited irregular and deeply net-like cracks (Fig. 17c) [46, 48]. These features differed markedly from the typical RCF damage morphology observed in actual rails (Fig. 1).

The D/W-A RCF testing method significantly enhanced the accuracy of simulating rail RCF damage under humid and rainy environments through the design of dry-wet alternating conditions.

This advantage was directly reflected in the high degree of consistency between the simulated RCF crack morphology and typical field RCF damage (Figs. 1 and 17d). Experimental results demonstrated that the D/W-A test not only reliably reproduced the full evolution process of RCF damage but also accurately captured the characteristic behaviors at different stages of crack propagation (Figs. 12 and 13). Moreover, wear behavior, plastic deformation accumulation, and crack propagation exhibited an interaction mechanism under dry-wet alternating conditions (Fig. 16). This provided a unique technical pathway for investigating the interplay of multiple damage modes in the wheel-rail system. It is worth noting that this accurate simulation came with increased system complexity of the test. However, as shown in Section 2, the integration of an automated dry-wet switching control system effectively improved the precision of condition transitions and enhanced overall test controllability.

To further evaluate the W, D-W, W, and D/W-A testing methods, a comprehensive evaluation of their performance was conducted across five dimensions: Accuracy, Repeatability, Evaluability, Rationality, and Practicability.

Firstly, the Accuracy of the testing method was aimed at assessing whether the testing method can accurately simulate the typical rail RCF damage. As illustrated in Fig. 17, both the D test and W test exhibited significant disparities in damage forms compared to typical RCF damage on rails. Particularly noteworthy was the W test, which was more suited for simulating RCF on continuously lubricated mechanical components. The D-W separated crack initiation and propagation, with an excessively fast propagation rate. It simulated the RCF damage of rail spalling to a considerable degree. Based on the rail damage behaviour in tests 4-7 (Fig. 12), the D/W-A test was particularly accurate in simulating RCF damage due to its ability to comprehensively model the entire process of wear, plastic deformation, crack initiation, and propagation.

Subsequently, the Reproducibility of the testing methods, specifically assessed to determine whether the operational process was conducive to repetition and whether artificial factors were likely to introduce interference into the test results. The D test exhibited the highest reproducibility in wear due to its stability and minimal operational steps. Although the W test was conducted under a single operating condition, test results tended to exhibit significant randomness. In the D-W test, the test under dry conditions could be regarded as the running-in test which the wheel-rail contact was not stable. Thus, a significant error would occur in the size of the initiated crack under dry condition, and then would have a significant impact on the subsequent crack propagation, leading to reduced reproducibility. Although the D/W-A test required frequent alternating conditions, the automation provided by the timed cycling controller will minimize the operational difficulty.

In terms of Evaluability, attention should be paid to the accessibility of evaluation indicators, the possibility of horizontal comparison, and their ability to reflect the true extent of damage. Due to the fact that the RCF life could be directly obtained with corresponding numerical results after the W test, without the need for complex measurements and calculations, the Evaluability of the W test proved to be the best. Other methods often relied on statistics of crack characteristics, among which the D test suffered from large measurement errors due to small crack sizes, while the D-W test posed difficulties in data acquisition because of the complex crack morphologies (Fig. 15). In the D/W-A test, there was a noticeable reduction in crack branching, which consequently diminished the difficulty of measurement, in comparison to the D-W test.

In terms of Rationality, it evaluated whether the test results could be reasonably explained. The fatigue life of the W test was difficult to represent the RCF life of unlubricated open components. The D test was mainly focused on wear, and crack statistics were insufficient to explain RCF damage. In the D-W test, cracks propagated into the material interior along plastic deformation and branched extensively, making the test rationality higher than the W test and D test. However, the complete separation of crack initiation and propagation led to a significant discrepancy compared to the actual crack propagation process in the rail. In the D/W-A test, it could observe different stages of crack propagation were observed, reflecting rail RCF damage behavior, especially under rainy and humid conditions.

Finally, in terms of Practicability, the test operation, duration, and labor costs were considered. The W test had the longest duration and the highest cost. The D test was the simplest to operate, and crack statistics were straightforward. However, the D-W and D/W-A tests required experienced operators, and crack statistics were relatively cumbersome.

Based on the comparison results from five dimensions, a radar chart was constructed, as illustrated in Fig. 18. In this chart, the method with the most significant advantage received a score of 5, the next best received a score of 4, and the least advantageous method received a score of 2. The D test demonstrates outstanding performance in terms of repeatability and practicability, but it has slight shortcomings in the other three dimensions. This testing method was commonly used to simulate the rolling wear of the rail. While the W test held the most significant advantage in evaluability, it lacked notable strengths in accuracy, rationality, and practicability when it came to simulating RCF. Meanwhile, the D-W test scored lower than the D/W-A test in Accuracy, Repeatability, and Rationality, while the scores were the same in the other two terms. As for the D/W-A test, it performed beyond other testing methods in terms of accuracy and rationality, while maintaining a certain level of competitiveness in the other three dimensions as well. This indicated that the overall performance of the D/W-A testing method was the best. Therefore, in the systematic study of RCF performance in rails, the D/W-A test proved to be a more effective tool.

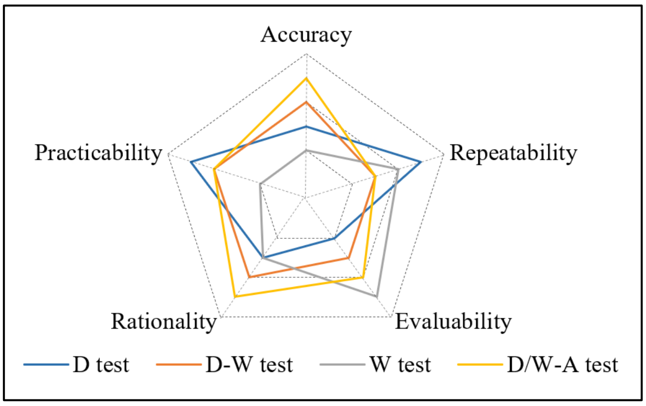


**Fig. 18.** Multi-dimensional evaluation of different RCF testing methods for rail and wheel materials.

Furthermore, due to the dynamic interaction among crack propagation, wear, and plastic deformation accumulation under dry-wet alternating conditions, in the future, the D/W-A method can be effectively used to quantitatively investigate the competitive relationship between wear and RCF. In addition, the evolution of RCF damage under the D/W-A testing method was controllable and stable, which greatly facilitated comparative studies on RCF damage characteristics across different wheel-rail materials. It also provided a reliable foundation for exploring the influence of RCF damage on other service behaviors of wheel-rail systems, such as plastic deformation, material hardening, corrosion, and adhesion.

## 5 Conclusion

(1) A novel wet-dry alternation testing method was proposed, to simulate RCF damage of rails, especially under rainy and humidity conditions.

(2) Under dry-wet alternation conditions, with increasing cycling number, RCF cracks initially propagated slowly along the plastic deformation direction and subsequently entered a stage of rapid propagation, gradually developing into "C" shaped cracks. During crack propagation, the rail material experienced continuous wear and accumulation of plastic deformation, which was in good agreement with the damage characteristics observed in actual rail service conditions.

(3) In the D test, cracks propagated within the SPD zone due to the lack of sufficient driving force for crack propagation. In the D-W test, cracks quickly passed through the SPD zone, generating numerous branches, and eventually forming a network of cracks. In the W test, cracks existed in a dense network formation with a mild degree of plastic deformation. In the D/W-A test, cracks propagated along the direction of plastic deformation with few branches.

(4) The D/W-A RCF test proposed in this study had significant advantages in rationality and accuracy compared with traditional RCF testing methods, providing a more effective tool for systematic studies on RCF performance of rail materials.

**Acknowledgements**

This work is supported by the National Natural Science Foundation of China (Nos. 52320105007, 52375205, 52575234) and Sichuan Province Innovative Talent Funding Project for Postdoctoral Fellows (No. BX202420).

**Declaration of competing interest**

The authors have no competing interests to declare that are relevant to the content of this article.

**References**

[1] Lian Q L, Deng G Y, Zhu H T, Li H J, Wang X, Liu Z M. Influence of white etching layer on rolling contact behavior at wheel-rail interface. *Friction* 8: 1178-96 (2020).

[2] Shen M X, Rong B, Li Q P, Yu M, Xiao Y L, Zhao H P. Different responses of wheel–rail interface adhesion and wheel surface damage induced by an out–of–round wheel tread. *Wear* 526-527: 204956 (2023).

[3] Hu Y, Zhou L, Ding H H, Tan G X, Lewis R, Liu Q Y, Guo J, Wang W J. Investigation on wear and rolling contact fatigue of wheel-rail materials under various wheel/rail hardness ratio and creepage conditions. *Tribology International* 143: 106091 (2020).

[4] Trummer G, Marte C, Dietmaier P, Sommitsch C, Six K. Modeling surface rolling contact fatigue crack initiation taking severe plastic shear deformation into account. *Wear* 352-353: 136-45 (2016).

[5] Tyfour W, Beynon J, Kapoor A. Deterioration of rolling contact fatigue life of pearlitic rail steel due to dry-wet rolling-sliding line contact. *Wear* 197: 255-65 (1996).

[6] Shen M X, Qin Y F, Ji D H, Yu M, Li S X, Huangfu L Z, Liu S P. Role of ambient temperature in the adhesion and damage characteristics of wheel/rail interface during rolling-sliding contact. *Wear* 506-507: 204458 (2022).

[7] Tunna I, Sinclair J, Perez J. A review of wheel wear and rolling contact fatigue. *Proceedings of the Institution of Mechanical Engineers, Part F: Journal of Rail and Rapid Transit* 221: 271-89 (2007).

[8] Santa J F, Toro A, Lewis R. Correlations between rail wear rates and operating conditions in a commercial railroad. *Tribology International* 95: 5-12 (2016).

[9] Jin X, Zhang J, Wen Z, Li F. Overview of phenomena of rolling contact fatigue of wheel/rail. *Journal of mechanical strength* 24: 250-7 (2002).

[10] Zhang H, Zhang S Y, Zhong H, Wang W, Meli E, Cui X, Ding H, Liu Q Y. Damage mechanism of a long-wavelength corrugated rail associated with rolling contact fatigue. *Engineering Failure Analysis* 136: 106173 (2022).

[11] Guo H M, Wang W J, Liu T F, Liu J H, Guo J, Liu Q Y. Analysis of damage behavior of heavy-haul railway rails. *China Mechanical Engineering* 25: 267-72 (2014).

[12] Chard A E Z. Deformation of inclusions in rail steel due to rolling contact [Ph.D]. United Kingdom: *University of Birmingham*; (2012).

[13] Huang Y B, Shi L B, Zhao X J, Cai Z B, Liu Q Y, Wang W J. On the formation and damage mechanism of rolling contact fatigue surface cracks of wheel/rail under the dry condition. *Wear* 400: 62-73 (2018).

[14] Liu C P, Zhao X J, Liu P T, Pan J Z, Ren R M. Influence of contact stress on surface microstructure and wear property of D2/U71Mn wheel-rail material. *Materials* 12: 3268 (2019).

[15] Liu C P, Zhao X J, Liu P T, Xu C, Ren R M. Influence of slip ratio on worn-surface microstructure and fatigue wear behavior of D2 wheel steel. *Journal of Iron and Steel Research International* 25: 1278-86 (2018).

[16] Zhao X J, Chen Q, Liu Y S, Qiu X Y, Meli E, Rindi A. Effects of slip ratio and contact stress on rolling contact fatigue of defected rail materials. *Engineering Failure Analysis* 131: 203254 (2022).

[17] Clayton P, Hill D N. Rolling contact fatigue of a rail steel. *Wear* 117: 319-34 (1987).

[18] Hu Y, Zhou L, Ding H H, Lewis R, Liu Q Y, Guo J, Wang W J. Microstructure evolution of railway pearlitic wheel steels under rolling-sliding contact loading. *Tribology International* 154: 106685 (2021).

[19] Bogdanski S, Brown M W. Modelling the three-dimensional behaviour of shallow rolling contact fatigue cracks in rails. *Wear* 253: 17-25 (2002).

[20] Bonniot T, Doquet V, Mai S H. Mixed mode II and III fatigue crack growth in a rail steel. *International Journal of Fatigue* 115: 42-52 (2018).

[21] Makino T, Kato T, Hirakawa K. The effect of slip ratio on the rolling contact fatigue property of railway wheel steel. *International Journal of Fatigue* 36: 68-79 (2012).

[22] Ringsberg J W, Bergkvist A. On propagation of short rolling contact fatigue cracks. *Fatigue & Fracture of Engineering Materials & Structures* 26: 969-83 (2003).

[23] Wang W J, Lewis S R, Lewis R, Beagles A, He C G, Liu Q Y. The role of slip ratio in rolling contact fatigue of rail materials under wet conditions. *Wear* 376: 1892-900 (2017).

[24] Zhao X J, Wang H Y, Guo J, Liu Q Y, Zhao G T, Wang W J. The effect of decarburized layer on rolling contact fatigue of rail materials under dry-wet conditions. *Engineering Failure Analysis* 91: 58-71 (2018).

[25] Liu X L, Zhao W, Cong T, Wang S G, Wang X, Wang W J. The effects of hardness on the spalling property of railway wheel steel. *Wear* 504: 204429 (2022).

[26] Zeng D F, Lu L T, Gong Y H, Zhang Y B, Zhang J W. Influence of solid solution strengthening on spalling behavior of railway wheel steel. *Wear* 372: 158-68 (2017).

[27] White B T, Nilsson R, Olofsson U, Arnall A D, Evans M D, Armitage T, Fisk J, Fletcher D I, Lewis R. Effect of the presence of moisture at the wheel–rail interface during dew and damp conditions. *Proceedings of the Institution of Mechanical Engineers, Part F: Journal of Rail and Rapid Transit* 232: 979-89 (2017).

[28] Shen M X, Li J Q, Li L, Li S X, Ma C Y. Adhesion and damage behaviour of wheel–Rail rolling–Sliding contact suffering intermittent airflow with different humidities and ambient temperatures. *Tribology Letters* 72: 18 (2024).

[29] Bodini I, Mazzù A, Petrogalli C, Lancini M, Kato T, Makino T. A study of wear and rolling contact fatigue on a wheel steel in alternated dry-wet contact aided by innovative measurement systems. *Procedia Structural Integrity* 18: 849-57 (2019).

[30] Zhang S Y, Spiryagin M, Ding H H, Wu Q, Guo J, Liu Q Y, Wang W J. Rail rolling contact fatigue formation and evolution with surface defects. *International Journal of Fatigue* 158: 106762 (2022).

[31] Li X C, Ding H H, Wang W J, Guo J, Liu Q Y, Zhou Z R. Investigation on the relationship between microstructure and wear characteristic of rail materials. *Tribology International* 163: 107152 (2021).

[32] Shu K, Wang W J, Ding H H, Lin Q, Meli E, Guo J, Mazzu A, Liu Q Y. Influence of sand transport rate on rolling wear and damage behaviors of wheel/rail in Gobi and desert windblown sand environments. *Tribology International* 172: 107584 (2022).

[33] Han Z Y, Wang H H, Wang W J, Zhang S Y, Lin D M, Wang Y, Ding H H, Zhou Z R, Liu Q Y. The correlation between material deformed microstructure and rolling contact fatigue crack propagation of U71Mn rail when matching with CL60 wheel. *Tribology International* 200: 110069 (2024).

[34] Wang Q, Wang Z, Mo J, Zhang L, Du L, Gou Q. Coupled dynamic behaviours of the brake system considering wheel–rail interactions. *International Journal of Rail Transportation* 10: 749-71 (2022).

[35] Wang H H, Wang W J, Han Z Y, Wang Y, Ding H H, Lewis R, Lin Q, Liu Q Y, Zhou Z R. Wear and rolling contact fatigue competition mechanism of different types of rail steels under various slip ratios. *Wear* 522: 204721 (2023).

[36] Song J D, Shi L B, Ding H H, Galas R, Omasta M, Wang W J, Guo J, Liu Q Y, Hartl M. Effects of solid friction modifier on friction and rolling contact fatigue damage of wheel-rail surfaces. *Friction* 10: 597-607 (2022).

[37] Zhou L, Wang W J, Hu Y, Marconi S, Meli E, Ding H H, Liu Q Y, Guo J, Rindi A. Study on the wear and damage behaviors of hypereutectoid rail steel in low temperature environment. *Wear* 456: 203365 (2020).

[38] Fukagai S, Brunskill H P, Hunter A K, Dwyer-Joyce R S, Lewis R. Transitions in rolling-sliding wheel/rail contact condition during running-in. *Tribology International* 149: 105679 (2020).

[39] Zhang R J, Zheng C L, Chen C, Lv B, Gao G H, Yang Z N, Yang Y Q, Zhang F C. Study on fatigue wear competition mechanism and microstructure evolution on the surface of a bainitic steel rail. *Wear* 482: 203978 (2021).

[40] Zhang S Y, Zhao H Y, Ding H, Lin Q, Wang W, Guo J, Wang P, Zhou Z. Effect of vibration amplitude and axle load on the rail rolling contact fatigue under water condition. *International Journal of Fatigue* 167: 107329 (2023).

[41] Leitner T, Trummer G, Pippan R, Hohenwarter A. Influence of severe plastic deformation and specimen orientation on the fatigue crack propagation behavior of a pearlitic steel. *Materials Science and Engineering: A* 710: 260-70 (2018).

[42] Wang Y P. Study on rolling contact fatigue shelling performance of wheel materials for high power locomotive: *Southwest Jiaotong University*; (2021).

[43] Han Z Y, Wang Y, Ding H H, Zhang S Y, Wang W J, Liu J P, Liu Q Y, Zhou Z R. Wear and Rolling Contact Fatigue Behavior of Pearlitic and Bainitic Rail Steels under Different Operating Parameters. *Tribology* 45: 1-12 (2025).

[44] Jia S F, Li Y Q, Zhou S B, Liu J P, Wang H H, Ding H H, Liu Q Y, Wang W J. Study on the Influence of Hardness Matching on Rolling Contact Fatigue Damage of Wheel-Rail Materials. *Materials Reports* 38: 415-21 (2024).

[45] Liu C P, Ren R M, Liu D Y, Zhao X J, Chen C H. An EBSD Investigation on the Evolution of the Surface Microstructure of D2 Wheel Steel During Rolling Contact Fatigue. *Tribology Letters* 68: 47 (2020).

[46] Wang Y P, Xiang P C, Ding H H, Wang W J, Zou Q, Liu X H, Guo J, Liu Q Y. Effects of molybdenum addition on rolling contact fatigue of locomotive wheels under rolling-sliding condition. *Materials* 13: 4282 (2020).

[47] Wang S s, Zhao X j, Liu P t, Pan J z, Chen C h, Ren R m. Investigation of the relation between rolling contact fatigue property and microstructure on the surface layer of D2 wheel steel. *Materials Sciences and Applications* 10: 509-26 (2019).

[48] Mazzu A, Petrogalli C, Lancini M, Ghidini A, Faccoli M. Effect of wear on surface crack propagation in rail-wheel wet contact. *Journal of Materials Engineering and Performance* 27: 630-9 (2018).



**Honghao WANG** PhD candidate. He received his Bachelor's degree in 2020 from Chongqing Jiaotong University and is currently pursuing a doctoral degree at Southwest Jiaotong University. His research interests include wheel/rail wear and rolling contact fatigue behavior. He has participated in many research projects and has published 7 papers in international journals during the past 3 years.

**Shuyue ZHANG**. She received her PhD degree in 2023 from Southwest Jiaotong University. Then she joined the Tribology Research Institute, State Key Laboratory of Rail Transit Vehicle System, Southwest Jiaotong University, China. Her current position is a lecturer. Her interested research areas include rail grinding, wheel-rail rolling contact fatigue behavior, wheel-rail simulation, etc.